Cancer Cell, *20*

Supplemental Information

Identification of *PHLPP1* as a Tumor Suppressor Reveals the Role of Feedback Activation in *PTEN*-Mutant Prostate Cancer Progression

Muhan Chen, Christopher P. Pratt, Martha E. Zeeman, Nikolaus Schultz, Barry S. Taylor, Audrey O'Neill, Mireia Castillo-Martin, Dawid G. Nowak, Adam Naguib, Danielle M. Grace, Jernej Murn, Nick Navin, Gurinder S. Atwal, Chris Sander, William L. Gerald, Carlos Cordon-Cardo, Alexandra C. Newton, Brett S. Carver and Lloyd C. Trotman

Supplemental Figures

Figure S1 is related to Figure 1.
Figure S2 is related to Figure 2.
Figure S3 is related to Figure 3.
Figure S4 is related to Figure 5.
Figure S5 is related to Figure 6.
Figure S6 is related to Figure 7.

Supplemental Experimental Procedures

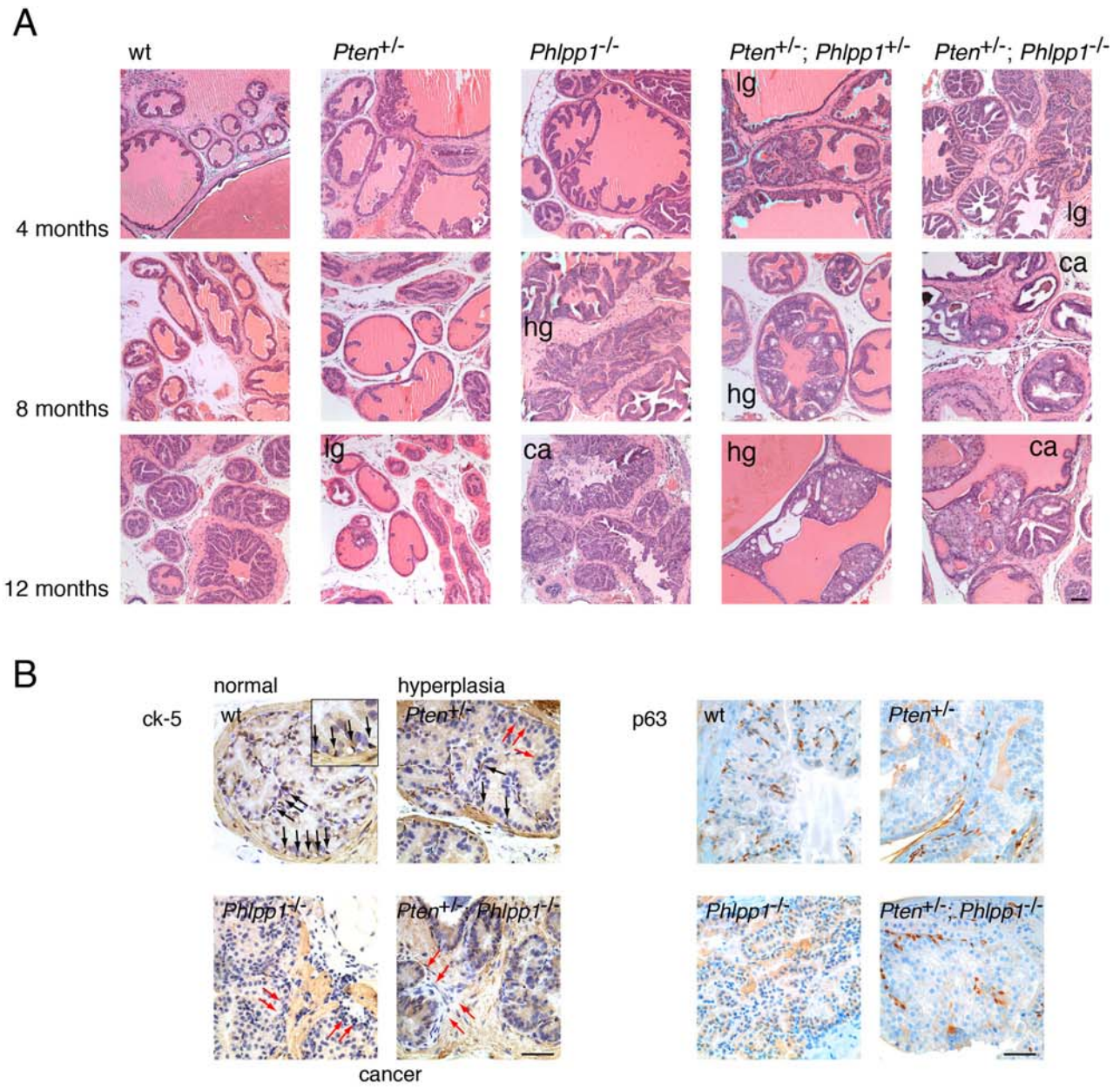
A
wt
Pten+/-
Phlpp1-/-
Pten+/-; Phlpp1+/-
Pten+/-; Phlpp1-/-
4 months
8 months
12 months
lg
hg
ca
B
normal
hyperplasia
ck-5
p63
wt
Pten+/-
Phlpp1-/-
Pten+/-; Phlpp1-/-
cancer
C
4 months
8 months
12 months
diameter in µm
700
525
350
175
0
wt
Pten+/-
Phlpp1-/-
Pten+/-; Phlpp1-/-
Pten+/-; Phlpp1+/-
12 months
D
apoptosis (cleaved caspase-3)
4m
8m
12m
percent positive cells
2.5%
2.0%
1.5%
1.0%
0.5%
0%
wt
Pten+/-
Phlpp1-/-
Pten+/-; Phlpp1-/-
Pten+/-; Phlpp1+/-
4.0%
3.0%
2.0%
1.0%
0%
immune response (Cd3)

Figure S1, related to Figure 1. Phenotypes of *Phlpp1*-loss *in vitro* and *in vivo*.

(A) Microscopic H&E analysis of 5 study cohort genotypes at indicated time points reveals cooperation between *Pten* and *Phlpp1*. Degree of malignancy for low grade-(lg) or high grade-(hg) PIN is shown for those ages and genotypes where at least 50% penetrance of PIN was found. Cases with adenocarcinoma (ca) are indicated (see Figure 1b for cancer penetrance and Experimental Procedures for animal numbers). Scale Bar, 50μm.

(B) Left panels, Cytokeratin 5 staining for basal epithelial cells shows progression from normal gland (frequent basal/ stalk staining, see black arrows) to hyperplasia in $Pten^{+/-}$ mice (partial loss, red and black arrows) and cancer (complete loss, red arrows) in $Phlpp1^{-/-}$ *and* $Pten^{+/-}$;$Phlpp1^{+/-}$ mice. Right panels, p63 staining of early neoplasia in indicated genotypes. Scale bars, 50μm.

(C) Quantification of lesion sizes over time reveals synergy between *Phlpp1*-loss and *Pten* heterozygosity (left graph). Error bars are s.d. of triplicates, p-values are < 0.002 and <0.006 for comparison of compound mutant ($Pten^{+/-}$; $Phlpp1^{-/-}$) with $Phlpp1^{-/-}$ or $Pten^{+/-}$, respectively at 8 months and p<0.006 and <0.003, respectively at 12 months. Right panel shows typical measurement of lesion size in $Pten^{+/-}$; $Phlpp1^{-/-}$ animal. Distance measured: 641.3 μm.

(D) Quantification of apoptosis (cleaved caspase 3 immunohistochemistry) reveals low levels in normal tissue and no decrease during malignancy (top). Quantification of immune response based on the T-lymphocyte marker Cd3 (bottom). Error bars are s.d. of triplicates.

A

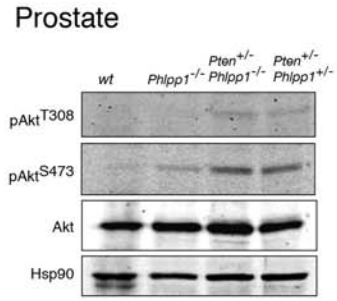
Prostate
wt
Phlpp1-/-
Pten+/- Phlpp1-/-
Pten+/- Phlpp1+/-
pAktT308
pAktS473
Akt
Hsp90

B

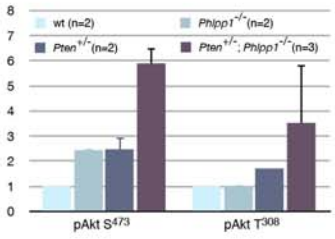
wt (n=2)
Phlpp1-/-(n=2)
Pten+/-(n=2)
Pten+/-; Phlpp1-/-(n=3)
pAkt S473
pAkt T308

C

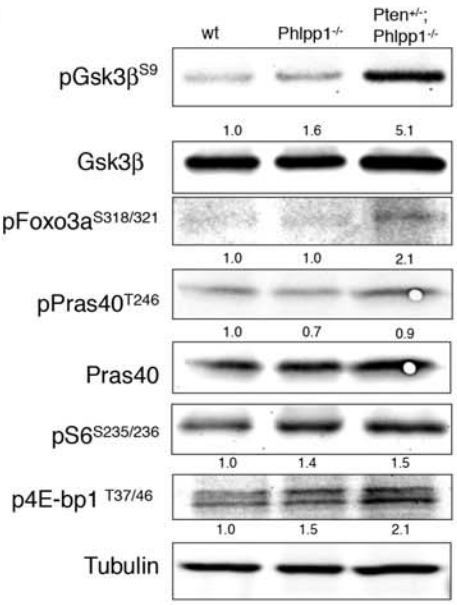
wt
Phlpp1-/-
Pten+/-; Phlpp1-/-
pGsk3βS9
1.0 1.6 5.1
Gsk3β
pFoxo3aS318/321
1.0 1.0 2.1
pPras40T246
1.0 0.7 0.9
Pras40
pS6S235/236
1.0 1.4 1.5
p4E-bp1 T37/46
1.0 1.5 2.1
Tubulin

D

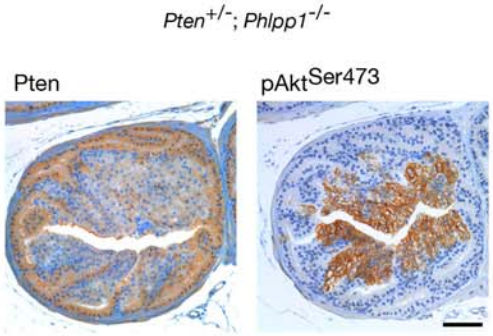
Pten+/-; Phlpp1-/-
Pten
pAktSer473

E

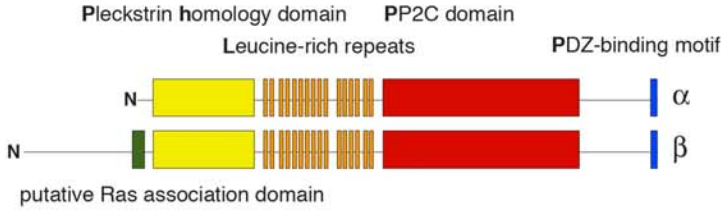
Pleckstrin homology domain
PP2C domain
Leucine-rich repeats
PDZ-binding motif
N
α
N
β
putative Ras association domain

Figure S2, related to Figure 2. Phlpp1 dose and Akt response *in vitro* and *in vivo*.

(A) Western blotting of Akt activation shows *Phlpp1*-dose dependent response on Ser^{473}: Note, that the $Pten^{+/-}$; $Phlpp1^{+/-}$ prostate reveals intermediate activation compared to $Phlpp1^{-/-}$ and $Pten^{+/-}$; $Phlpp1^{-/-}$.

(B) Averaged quantification of Akt activation in WT, $Pten^{+/-}$, $Phlpp1^{-/-}$, and $Pten^{+/-}$; $Phlpp1^{-/-}$ prostates on both activation sites. Error bars are s.d. of triplicates.

(C) Western blotting and quantification of downstream Akt target activation in 6 month old prostates from indicated genotypes.

(D) Pten IHC staining illustrates gland with spontaneous drop of Pten protein at 8 months in $Pten^{+/-}$;$Phlpp1^{-/-}$ prostate (left panel). IHC staining on a serial section reveals inversely correlated Akt activation (Ser^{473}, right panel). Scale bar, 100 μm.

(E) Domain organization of the two PHLPP1 protein isoforms. PHLPP1α and PHLPP1β are equally expressed in the PC3 human prostate cancer cell line. Phlpp1α expression patterns in mouse have to date not been determined.

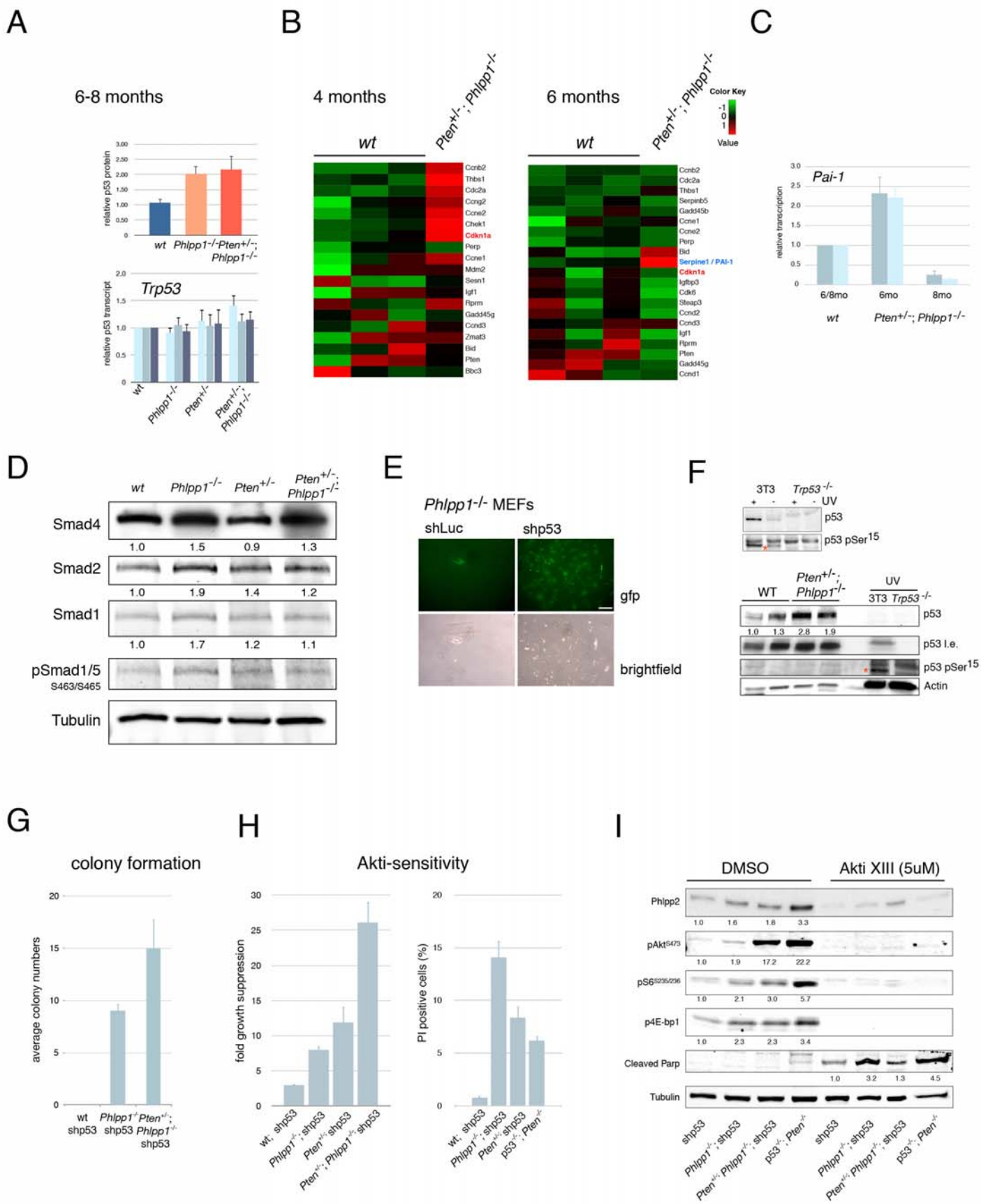
A
6-8 months
relative p53 protein
wt
Phlpp1-/-
Pten+/-;
Phlpp1-/-
Trp53
relative p53 transcript
wt
Phlpp1-/-
Pten+/-
Pten+/-;
Phlpp1-/-
B
4 months
wt
Pten+/-; Phlpp1-/-
Ccnb2
Thbs1
Cdc2a
Ccng2
Ccne2
Chek1
Cdkn1a
Perp
Ccne1
Mdm2
Sesn1
Igf1
Rprm
Gadd45g
Ccnd3
Zmat3
Bid
Pten
Bbc3
6 months
wt
Pten+/-; Phlpp1-/-
Color Key
Value
Ccnb2
Cdc2a
Thbs1
Serpinb5
Gadd45b
Ccne1
Ccne2
Perp
Bid
Serpine1 / PAI-1
Cdkn1a
Igfbp3
Cdk6
Steap3
Ccnd2
Ccnd3
Igf1
Rprm
Pten
Gadd45g
Ccnd1
C
Pai-1
relative transcription
6/8mo
6mo
8mo
wt
Pten+/-; Phlpp1-/-
D
wt
Phlpp1-/-
Pten+/-
Pten+/-;
Phlpp1-/-
Smad4
1.0 1.5 0.9 1.3
Smad2
1.0 1.9 1.4 1.2
Smad1
1.0 1.7 1.2 1.1
pSmad1/5
S463/S465
Tubulin
E
Phlpp1-/- MEFs
shLuc
shp53
gfp
brightfield
F
3T3
Trp53 -/-
+ - + - UV
p53
p53 pSer15
WT
Pten+/-;
Phlpp1-/-
UV
3T3
Trp53 -/-
p53
1.0 1.3 2.8 1.9
p53 l.e.
p53 pSer15
Actin
G
colony formation
average colony numbers
wt
shp53
Phlpp1-/-
shp53
Pten+/-;
Phlpp1-/-
shp53
H
Akti-sensitivity
fold growth suppression
wt; shp53
Phlpp1-/-; shp53
Pten+/-; shp53
Pten+/-; Phlpp1-/- shp53
PI positive cells (%)
wt; shp53
Phlpp1-/-; shp53
Pten+/-; shp53
p53-/-; Pten-/-
I
DMSO
Akti XIII (5uM)
Phlpp2
1.0 1.6 1.8 3.3
pAktS473
1.0 1.9 17.2 22.2
pS6S235/236
1.0 2.1 3.0 5.7
p4E-bp1
1.0 2.3 2.3 3.4
Cleaved Parp
1.0 3.2 1.3 4.5
Tubulin
shp53
Phlpp1-/-; shp53
Pten+/-; Phlpp1-/-; shp53
p53-/-; Pten-/-
shp53
Phlpp1-/-; shp53
Pten+/-; Phlpp1-/-; shp53
p53-/-; Pten-/-

Figure S3, related to Figure 3. p53-dependent growth arrest in *Phlpp1*$^{-/-}$ MEFs.

(A) Average p53 protein levels (top) at 6-8 months of age in prostates of WT (n=4), *Phlpp1*$^{-/-}$ (n=2), *Pten*$^{+/-}$;*Phlpp1*$^{-/-}$ mice (n=4). Bottom panel: RT-qPCR of *Trp53* mRNA levels in prostates from Figure 3A and indicated genotypes. Colors represent different primer pairs. Error bars are s.d. of triplicates.

(B) Transcriptional profiling of p53 target genes using microarrays of prostates shown in Figures 3C-D reveals decreased expression profile at 6 months in the compound mutant.

(C) RT-qPCR of *SerpinE1/ Pai-1* mRNA levels in prostates from indicated genotypes and ages reveals transient activation (6 months) and strongly reduced transcription at 8 months. Colors represent different primer pairs. Error bars are s.d. of triplicates.

(D) Tgf-beta pathway activation is found in *Phlpp1*$^{-/-}$ (*Pten*$^{+/-}$) Western blotting and quantification of Smad1, Smad2, and Smad4 levels in 6 month old prostates from indicated genotypes.

(E) Colony outgrowth in arrested *Phlpp1* null MEFs after infection with shp53 or control RNAi at 16 days post-infection. Note that phase contrast images reveal absence of RNAi-positive clones growing in the control infection. Scale Bar, 50μm.

(F) *Pten*$^{+/-}$; *Phlpp1*$^{-/-}$ prostate shows increased p53 but not p53 phosphorylation at serine 15 (Ser^{15}). Red asterisk shows location of the band for phospho-Ser^{15}. Note the absence of phospho-Ser^{15} in prostate and high ratio of phospho-Ser^{15} to p53 in the NIH-3T3 positive control (UV) compared to prostate. l.e. denotes long exposure.

(G) Quantification of colony formation assays for shp53 MEFs of indicated genotypes. Error bars are s.d. of triplicates.

(H) Sensitivity of Akt inhibition in shp53 from Figure 4E. Left panel, fold change in growth suppression upon Akt-inhibitor treatment, compared to DMSO treatment at day 7. Error bars are s.d. of quadruplicates. Right panel, quantification of cell death (propidium iodide positive percentage) upon Akt-inhibitor treatment for 6 hours. Error bars are s.d. of triplicates.

(I) Western blotting and quantification of Akt pathway inhibition and of Parp cleavage in indicated MEFs.

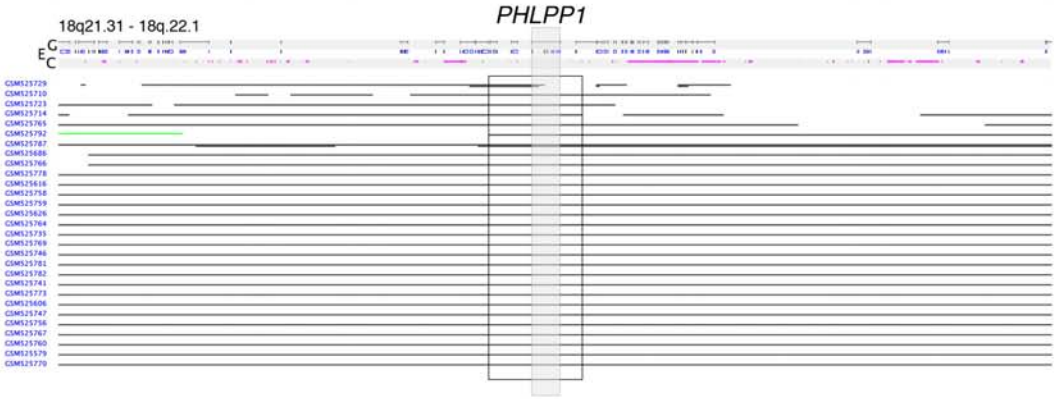
18q21.31 - 18q.22.1
PHLPP1

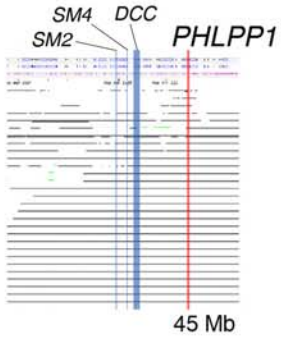
SM4
DCC
SM2
PHLPP1
45 Mb

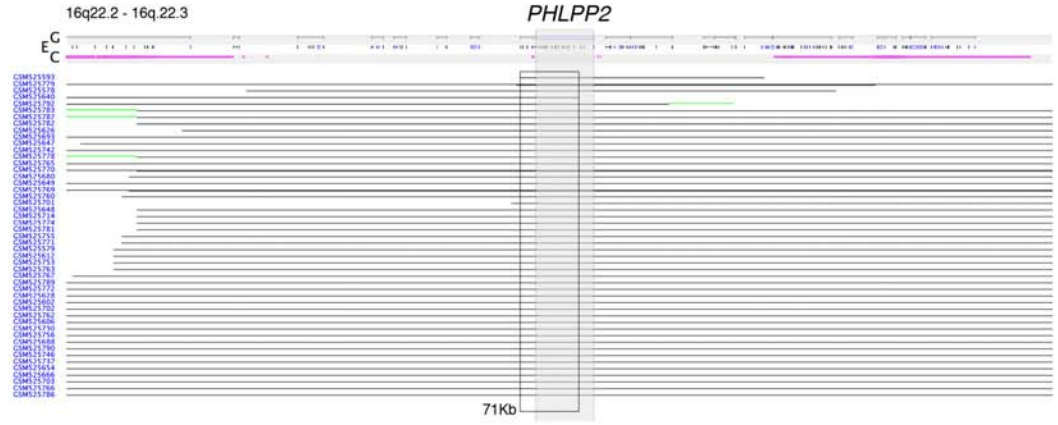
16q22.2 - 16q.22.3
PHLPP2
71Kb


PHLPP2
4.8 Mb

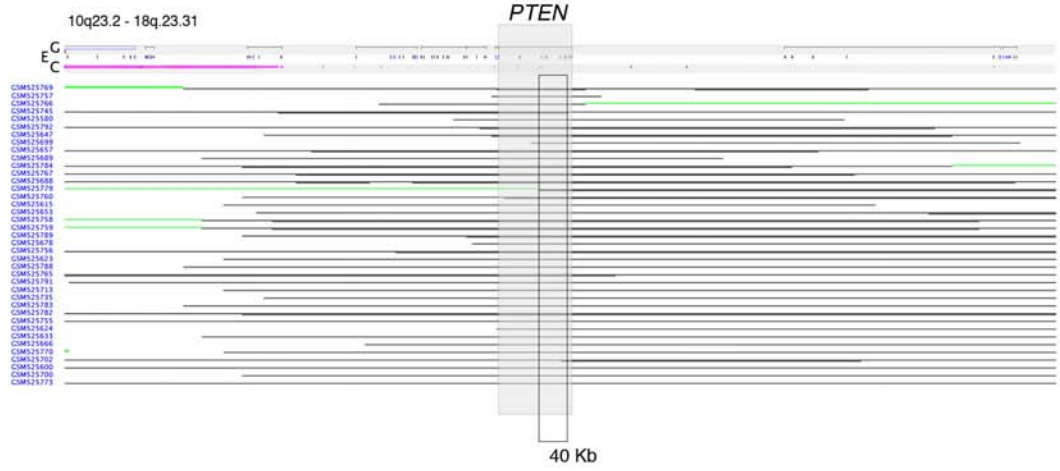
10q23.2 - 18q.23.31
PTEN
40 Kb


PTEN
13.2 Mb

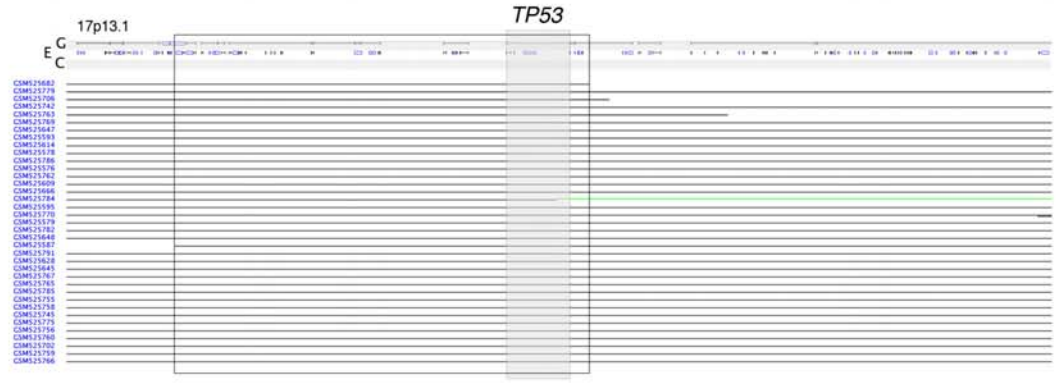
17p13.1
TP53


TP53
4.5 Mb

Figure S4, related to Figure 5. Overview of deleted regions in prostate cancer.

Left panels: summary of the deletions and common deleted regions (CDRs) of the *PHLPP1*, *PHLPP2*, *PTEN* and *TP53* loci in the entire patient sample set. Gene locations are indicated and boxed (grey), CDRs are boxed and sizes are indicated. Tracks with location of genes (G), Exons (E) and known Copy Number Variations (C) are shown. Heterozygous (grey) and homozygous deletions (bold) and amplifications (green) are shown. Note that the *PHLPP1* CDR contains only 3 other genes without known or putative tumor suppressor function. Right Panels: Overview of the gene loci and deletion sizes. Locations and common deletions between *SMAD2* (SM2), *SMAD4* (SM4), *DCC* and *PHLPP1* are shown.

A

deletion vs. expression

Gene	low expression/ deletion	suppression/ deletion percent	*p-value*
SMAD4	11/17	65%	*1.9E-07*
PHLPP1	13/18	72%	*8.1E-07*
PTEN	12/22	55%	*3.6E-05*
PHLPP2	7/34	21%	*6.0E-03*
TP53	5/25	20%	*4.3E-02*
DCC	4/18	22%	*2.6E-01*

B

PTEN deletion

Event	associated events	total events	percentage in PTEN group	*p* value
TP53 **deletion**	17	37	46%	*6.2E-06*
PHLPP1 **deletion**	13	29	45%	*1.8E-04*
SMAD4 **deletion**	12	26	46%	*2.5E-04*
DCC **deletion**	13	30	43%	*2.8E-04*
PHLPP2 **deletion**	16	50	32%	*2.9E-03*
AKT1 amplification	10	35	29%	*5.4E-02*
MYC amplification	12	49	24%	*1.1E-01*
FOXO3a deletion	11	48	23%	*1.8E-01*

low PTEN expression

Event	associated events	total events	percentage in PTEN group	*p* value
SMAD4 **low expression**	15	21	54%	*7.0E-09*
PTEN **deletion**	12	22	43%	*3.6E-05*
PHLPP1 **low expression**	14	32	50%	*1.5E-04*
PHLPP2 **low expression**	6	12	21%	*1.0E-02*
TP53 low expression	4	13	14%	*2.0E-01*
MYC amplification	8	34	29%	*2.8E-01*
FOXO3 deletion	7	34	25%	*4.6E-01*
DCC low expression	4	22	14%	*6.3E-01*
AKT1 amplification	2	20	7%	*9.3E-01*

C

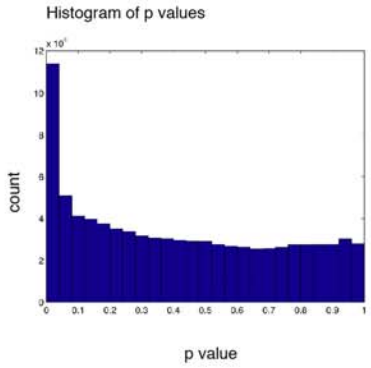

D

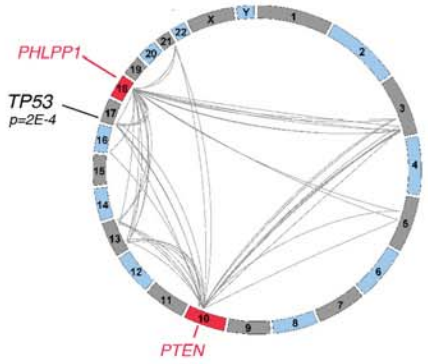

E

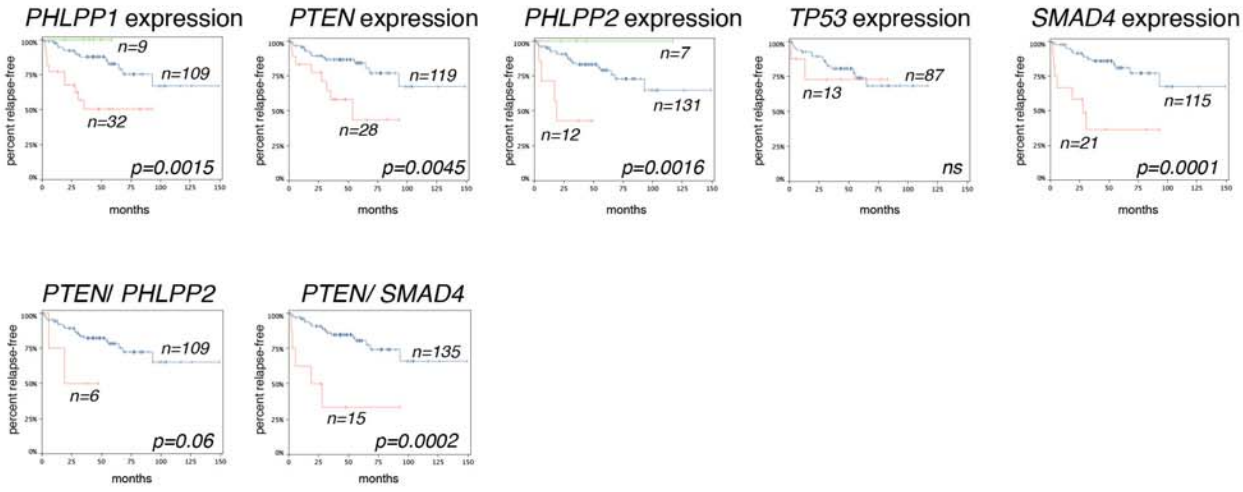

Figure S5, related to Figure 6. Expression correlations and prognosis.

(A) Table for deletion:expression correlation of genes of interest from 150 samples. Statistical significance of overrepresentation of low expression for a gene in its deleted set was calculated using a two-tailed Fisher's exact test. Note that the correlations for *TP53* and *DCC* are weakest.

(B) Correlation tables for deletion (top) and low expression (bottom) of *PTEN* and indicated genes in 218 human prostate cancer samples. Note that some validated prostate cancer alterations (*AKT1*-, *MYC*-amplification, *FOXO3a*-deletion) do not correlate with *PTEN* status.

(C) Histogram of the p-values calculated for significance of co-deletion of all possible pairs among deleted genes in metastasis (see Experimental Procedures). Note that *PTEN*, *PHLPP1*/*2* and *TP53* co-deletions fall into the leftmost bin of non-randomly associated gene deletions ($0 < p \leq 0.4$).

(D) Circos plot of genome-wide co-deletion events in *PTEN*/ *PHLPP1* double-mutant metastatic samples at a cutoff of p=0.005 reveals significant association of these two events with *TP53*-loss at 17p *(*p=2E-4).

(E) Kaplan-Meier curves for outcome prediction of indicated genes (top) or gene pairs (bottom). Low (red) and normal (blue) expressing samples are shown. Note that only significantly different high expression curves are shown (green).

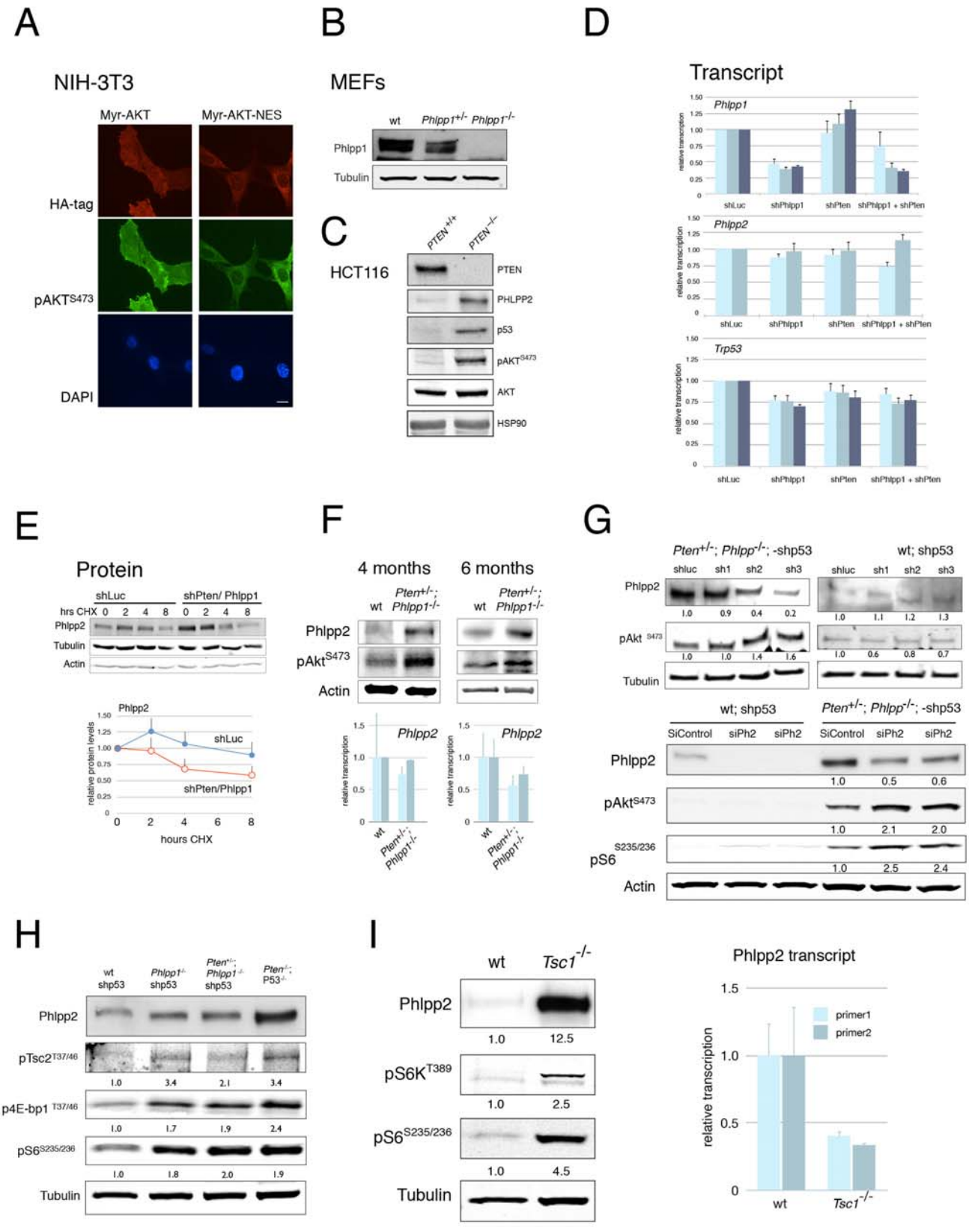
A
NIH-3T3
Myr-AKT
Myr-AKT-NES
HA-tag
pAKTS473
DAPI
B
MEFs
wt
Phlpp1+/-
Phlpp1-/-
Phlpp1
Tubulin
C
HCT116
PTEN+/+
PTEN-/-
PTEN
PHLPP2
p53
pAKTS473
AKT
HSP90
D
Transcript
Phlpp1
Phlpp2
Trp53
relative transcription
shLuc
shPhlpp1
shPten
shPhlpp1 + shPten
E
Protein
shLuc
shPten/ Phlpp1
hrs CHX 0 2 4 8 0 2 4 8
Phlpp2
Tubulin
Actin
relative protein levels
hours CHX
F
4 months
6 months
Pten+/-; Phlpp1-/-
Phlpp2
pAktS473
Actin
relative transcription
G
Pten+/-; Phlpp-/-; -shp53
wt; shp53
shluc
sh1
sh2
sh3
Phlpp2
pAkt S473
Tubulin
SiControl
siPh2
pAktS473
pS6 S235/236
Actin
H
wt shp53
Phlpp1-/- shp53
Pten+/-; Phlpp1-/- shp53
Pten-/-; P53-/-
Phlpp2
pTsc2T37/46
p4E-bp1 T37/46
pS6S235/236
Tubulin
I
wt
Tsc1-/-
Phlpp2
pS6KT389
pS6S235/236
Tubulin
Phlpp2 transcript
primer1
primer2
relative transcription

Figure S6, related to Figure 7. Feedback activation after *Pten*/ *Phlpp1*-loss.

(A) The Myr-AKT-NES plasmid shows nuclear exclusion of active pAKT^{S473}. Scale Bar, 10μm.

(B) The human anti-PHLPP1 antibody recognizes mouse Phlpp1 protein in Western analysis.

(C) The human HCT-116 *PTEN* knockout cell line shows PHLPP2 and p53 activation.

(D) RT-qPCR reveals no change in *Phlpp2* or *Trp53* mRNA. Colors represent different primer pairs. Error bars are s.d. of triplicates.

(E) Western analysis (top) and the quantification (bottom) of Phlpp2 protein turnover using cycloheximide (CHX) shows no surge in protein levels but rather decreased Phlpp2 stability in the *Pten*/ *Phlpp1* knockdown cells. Error bars are s.d. of triplicates

(F) Top panel, Western blotting and quantification of Phlpp2 and pAkt Ser^{473} in prostates of indicated ages and genotypes. Bottom panel, RT-qPCR of *Phlpp2* transcripts on prostates from top. Colored bars represent different primer pairs. Error bars are s.d. of triplicates.

(G) Western blotting of pAkt Ser^{473} status reveals Akt (and Rp-S6) activation after suppressing the Phlpp2 surge by knockdown with three different shRNAs (top panels) or 2 different siRNAs (bottom panels) in *Pten*$^{+/-}$; *Phlpp1*$^{-/-}$; shp53 MEFs.

(H) Western blotting and quantification of Akt downstream targets Tsc2, S6, 4Ebp1 and Phlpp2 in MEFs of indicated genotypes.

(I) Left panel, Western blotting and quantification of high Phlpp2 level and Akt pathway activation in *Tsc1*$^{-/-}$ MEFs. Right panel, RT-qPCR of *Phlpp2* transcripts on MEFs from left panel. Colored bars represent different primer pairs. Error bars are s.d. of triplicates.

Supplemental Experimental Procedures

Western blotting antibodies

Western Blotting was done using the following polyclonal antibodies from Cell Signaling (product number): Phospho-Akt Ser^{473} (#9271 & #4051), Phospho-Akt Thr^{308}, (#9275 & #2965), Akt (#9272), Phospho-Erk1/2 (Thr$^{202/}$Tyr^{204}, #4377), anti-Erk1/2 (#4695), Phospho-MEK1/2 (Ser^{217}/^{221}, #9154), anti-MEK (#4694), Phospho-p70 S6 kinase (Thr^{389}, #9205), Phospho-S6 ribosomal protein Ser$^{235/236}$(#4856), HSP90 (#4874), Phospho-Smad1/5 Ser$^{463/465}$ (#9516), Smad1 (#6944), Smad2 (#5339), Phospho-Smad2 Ser$^{465/467}$ (#3108), Smad3 (#9523), Phospho-Smad3 Ser$^{423/425}$ (#9520), Smad5 (#9517), Phospho-PRAS40 Thr^{246} (#2997), PRAS40 (#2691), Phospho-GSK-3α/β Ser$^{21/9}$ (#9331), GSK-3β (#9315), Phospho-Tuberin/TSC2 Thr^{1462} (#3617), Tuberin/TSC2 (#3990), Phospho-FoxO3a Ser$^{318/321}$ (#9465), FoxO3a (#2497), Phospho-4E BP1 Thr$^{37/46}$ (#9459), PARP (#9542).

The following Cell Signaling phospho-p53 antibodies were also used: Ser^{6} (#9285), Ser^{9} (#9288), Ser^{15} (#9284), Ser^{20} (#9287), Ser^{37} (#9289), Ser^{46} (2521), and Ser^{392} (#9281). Other polyclonal antibodies used were: PHLPP1 (IHC-00382, Bethyl Lab), PHLPP1 (BL2678) (A300-659A, Bethyl Lab), PHLPP2 (A300-661A, Bethyl Lab), p21 (SC-397, Santa Cruz), Smad4 (SC-7966, Santa Cruz), and PCNA (SC-56, Santa Cruz). Monoclonal antibodies used were p53 (Clone IMX25, Accurate Chemical Corp), Pten (Clone 6H2.1, Millipore), beta-Actin (A5441, Sigma) and gamma-Tubulin (T6199, Sigma). Western blots were developed using the enhanced chemiluminescence detection reagent (Millipore) and the Odyssey Infrared Imaging System (Li-Cor). Quantification of densitometry was performed using ImageJ 1.38X (NIH) software.

Immunohistochemistry (IHC), Quantifications, senescence associated β-gal staining, and Immunofluorescence (IF)

Tissues were fixed in 10% formalin and embedded in paraffin. Sections were processed with H&E reagents or stained for phopho-Akt (Ser^{473}, IHC-specific, #4060, Cell signalling), PTEN/MMAC1 Ab-2 (#RB-072-PO, NeoMarkers), PHLPP1 (IHC-00382,

Bethyl Lab, 1:700 dilution), Ki-67 (VP-K451, Vector Labs), p53 (FL-393, Santa Cruz), p63 (4A4, Santa Cruz), Cleaved Caspase 3 (#9661, Cell Signaling), CD3 (#A0452, Dako), or Cytokeratin 5 (AF-138, Covance) using Discovery XT processor (Ventana Medical Systems) as previously described (Trotman et al., 2003). The slides were processed using citrate buffer (10mM, ph=6.0) based antigen retrieval, and the avidin-biotin peroxidase IHC method. Quantification of malignancy was done as follows: for Ki-67 staining cells were counted after imaging with a Zeiss Axioplan microscope (40x objective). Numbers of mice (n), histology sections/ animal (s), and cells counted/ section (c) were: WT, n=3, s=4, c=630. *Pten*$^{+/-}$, n=3, s=6, c=907. *Phlpp*$^{-/-}$, n=3, s=6, c=1429. *Pten*$^{+/-}$; *Phlpp*$^{-/-}$, n=5, s=9, c=1976. *Pten*$^{+/-}$; *Phlpp*$^{+/-}$, n=6, s=8, c=1592.

For apoptosis (cleaved caspase 3) and immune response (Cd3) between 500-1500 cells total were counted on 4 sections per genotype and age. For lesion size, straight lines forming the maximal diameter of a neoplasia were drawn using the measurement tool of the SPOT microscopy imaging software (www.diaginc.com) on 4 sections per genotype and age. Statistical analysis was performed using the one-tailed student's t-test. Frozen sections were fixed in 0.5% glutaraldehyde, followed by wash with PBS, then PBS/$MgCl_2$ (pH 5.5). Fresh X-gal staining solution (Roche) was applied, and the slides were incubated at 37˚C. Then the slides were washed with PBS twice, fixed with 4% formalin, and counter-stained with eosin.

For IF, cells were seeded on glass cover slips in 24-well plates and fixed with 4% para-fomaldehyde for 10 min followed by 50 mM NH_4Cl for 10 min, 0.5% Triton X-100 for 5 min, and PBS (3 times wash), 10% goat serum (30 min) and primary antibodies hemagglutinin (HA) (Clone 12CA5, CSHL monoclonal antibody core) and phopho-Akt (Ser^{473}, IHC-specific, #4060, Cell Signaling), were applied for 5 hours at 4 degrees or as indicated by the manufacturer.

Secondary antibodies were goat anti-rabbit and goat anti-mouse Alexa 546 or 488 (Invitrogen-Molecular Probes, IMP), and DAPI (1:500, Sigma) was used for identification of cell nuclei. Cover slips were mounted using ProLong Gold antifade reagent (P36930, Invitrogen) and sealed with clear nail polish after curing at room temperature. Confocal

analysis was performed on a Perkin Elmer Spinning Disk Confocal Microsope using Volocity software v. 5.3.0.

Cells, Infection and Treatment

MEFs were isolated as previously described (Trotman et al., 2006) from individual embryos of various genotypes, and cultured in 10% fetal bovine serum in DMEM (with antibiotics and Glutamine). Primary MEFs at passage 3 or stable cell lines were plated in triplicates at 1.25 x 10^4 cells per well in 12- well plates for determination of growth curves by spectroscopic measurement of crystal violet uptake. For retroviral infection, Phoenix cells were plated and transfected with the non-mammalian control short hairpin against firefly Renilla Luciferase or short hairpin p53.1224 (see below) by the calcium phosphate method. After 48 hours, the virus-containing medium was filtered (0.45 μm filter, Millipore) and supplemented with 4 μg/ml polybrene (Sigma) and applied to the MEFs. These hairpins co-express GFP as marker of infection. To assess GFP enrichment over time, GFP positive cells were measured by flow cytometry using the Guava easyCyte 8HTsystem (Millipore) on days 1, 12, 16, and 20 and normalized relative to the gfp-positive cell number at day 1. These day 1 averages were 800 cells (wt), 1425 cells (*Phlpp1*$^{-/-}$), and 2525 (*Pten*$^{+/-}$; *Phlpp1*$^{-/-}$) cells irrespective of infection with shluc or shp53 virus).

For soft agar assay, primary MEFs and selected MEFs were suspended in medium containing 0.3% agar onto solidified 0.6% agar at a concentration of 1 x 10^4 cells per well of a six-well plate, and the number of colonies was assessed after 21 days. For Akt inhibition, cells were treated with 5uM AKT inhibitor XIII (Calbiochem, Cat# 124017) for 6 hours and harvested for western blot analysis and viability assay. To assess cell viability, cells were stained with Propidium iodide (Millipore) and PI positive cells were measured by flow cytometry using the Guava easyCyte 8HTsystem (Millipore). For mTOR inhibition, cells were treated with 100 nM rapamycin (LC Laboratories) for 24 hours and harvested for western blot analysis. NIH3T3 and MEFs were treated with UV at the dose of 50 J/m at 245nm and harvested 24 hours post treatment. To determine protein half-life, 1 x 10^6 cells were seeded on 10cm dishes, treated with 100 mg/ml

cycloheximide (Calbiochem) and harvested at the indicated times for western blot analysis. *Pten*/ *Trp53* deleted MEFs were previsously described (Chen et al., 2005). HCT116 *PTEN*$^{+/+}$ and HCT116 *PTEN*$^{-/-}$ (KO22) cells were a kind gift from Dr. Todd Waldman (Kim et al., 2006). *Tsc1*$^{-/-}$ MEFs were a kind gift from Dr. David Kwiatkowski (Kwiatkowski et al. 2002).

RNA expression array analysis

RNA quality was assessed on an Agilent 2100 Bioanalyzer, RNA 6000 Pico Series II Chips (Agilent, Palo Alto, CA, USA). Samples with a RIN score 2.0 or greater were passed, and quantity was determined by Nanodrop ND-1000 (Nanodrop Technologies, Wilmington, DE). Total RNA was amplified by a modified Eberwine Technique, and aRNA converted to cDNA using the WT Expression kit (Ambion, Austin, TX, see Van Gelder RN *et al. Proc Natl Acad Sci USA*, 1990, 87: 1663-1667.**)**. Size distribution of aRNA and cDNA was assessed and 3' bias was performed on all samples and products using the Agilent 2100 Bioanalyzer RNA 6000 Nano Series II Chips (Agilent, Palo Alto, CA, USA). The cDNA was then fragmented and terminally labeled with biotin, using the Affymetrix GeneChip WT Terminal Labeling kit (Affymetrix, Santa Clara, CA). Samples were prepared for hybridization, hybridized, washed, and scanned according to the manufacturer's instructions on Mouse Gene ST 1.0 GeneChips (Affymetrix, Santa Clara, CA). Affymetrix Expression Console QC metrics were used to pass the image data.

Quantitative real time PCR

RNA was isolated from tissue (AllPrep) or cells (Trizol method, Ambion), and cDNA was produced from 2ug of RNA using the SuperScript III system with oligo dT primers (Invitrogen) as suggested by the manufacturer. Quantitative real-time PCR was performed on the LightCycler 480 Real-Time PCR System using the SYBR Green I Master (Roche) and the following amplification protocol: 5 min at 95°C, 40 cycles (15 sec at 94°C - 10 sec at 60°C - 10 sec at 72°C) followed by determination/confirmation of amplicon melting temperature. Reactions were performed in triplicates, 3 primer pairs for each gene were confirmed to yield a single amplicon band by 2% agarose gel

electrophoresis. Absence of amplification from non reverse-transcribed RNA was confirmed to exclude genomic DNA amplification. Quantifications were done using the LightCycler 480 Relative Quantification Software. The mouse primer sets used were obtained from PrimerBank (http://pga.mgh.harvard.edu/primerbank): p53 (PrimerBank ID: 6755881a), pair 1, Fwd1 (5'-GCGTAAACGCTTCGAGATGTT-3'), Rev1 (5'-TTTTTATGGCGGGAAGTAGACTG-3'), pair 2, Fwd2 (5'-GTCACAGCACATGACGGAGG-3'), Rev2 (5'-TCTTCCAGATGCTCGGGATAC-3'), pair 3, Fwd3 (5'-CTCTCCCCCGCAAAAGAAAAA-3'), Rev3 (5'-CGGAACATCTCGAAGCGTTTA-3'); p21 (PrimerBank ID: 6671726a), pair 1, Fwd1 (5'-CCTGGTGATGTCCGACCTG-3'), Rev1 (5'-CCATGAGCGCATCGCAATC-3'), pair 2, Fwd2 (5'-CGAGAACGGTGGAACTTTGAC -3'), Rev2 (5'-CAGGGCTCAGGTAGACCTTG-3'); Phlpp1 (PrimerBank ID: 26006185a), pair 1, Fwd1 (5'- AGGGTCCCGGAGACGATAAG-3'), Rev1 (5'-AGGGCGGAGATGTCTTTTGC-3'), pair 2, Fwd2 (5'-ATCTCCGCCCTCCCTGTATG-3'), Rev2 (5'-GAATGAGACAGCCAATCTCTGAG-3'), pair 3, Fwd3 (5'-GATTGGCTGTCTCATTCGATTCT-3'), Rev3 (5'-GTCCATCGGTTCACTGGCAA-3'); Phlpp2 (PrimerBank ID: 26339234a), pair 1, Fwd1 (5'-GCCACAATCTTCTTACAGAGGTC-3'), Rev1 (5'-TCGAGGGGAATGTGCTCCA-3') pair 2, Fwd2 (5'-TCCAGCATAACACTCTCTCCA-3'), Rev2 (5'-GCAGCACACTCAGACTCTCC-3'), pair 3, Fwd3 (5'-CTGACAGATCAGTGCATACCAG-3'), Rev3 (5'-TTGTTCCCACTTAGATTCAGCTC-3'); Pai1 (PrimerBank ID: 6679373a1) pair 1, Fwd1 (5'-TTCAGCCCTTGCTTGCCTC-3'), Rev1 (5'-ACACTTTTACTCCGAAGTCGGT-3') pair 2, Fwd2 (5'-TTCGGAGTAAAAGTGTTTCAGCA-3'), Rev2 (5'-TGAGCTGTGCCCTTCTCATTG-3'); and Hprt1 (PrimerBank ID: 7305155a), Fwd (5'-TCAGTCAACGGGGGACATAAA-3'), and Rev (5'-GGGGCTGTACTGCTTAACCAG-3').

Sequencing of *Trp53* cDNA

RNA was isolated simultaneously with protein and DNA using Allprep DNA/RNA/Protein kit (Qiagen) and cDNA was synthesized (as described above) from mouse prostates of

the following genotypes and ages: 6 *Pten*$^{+/-}$; *Phlpp1*$^{-/-}$ animals (2-11 months), 1 *Phlpp1*$^{-/-}$ animal (6 months), 2 wt animals (4 and 8 months), 1 *Pten*$^{+/-}$; *Phlpp1*$^{+/-}$ animal (10 months), 1 *Pten*$^{+/-}$; animal (8 months), as well as from low passage primary *Phlpp1*$^{-/-}$ MEFs, and cDNA was synthesized as described above. Full-length p53 transcripts were amplified to yield three Sanger sequencing compatible fragments using three primer pairs: pair 1, Fwd1 (5'- TTTCCCCTC CCACGTGCTCACCCTGG -3'), Rev1 (5'- CGGAGCAGCGCTCATGGTGGGGGCAGC G -3'), pair 2, Fwd2 (5'- CCGCGCCAT GGCCATCTACAAG -3'), Rev2 (5'- CTCTAAGGCCTCATTCAGCTCCCGG -3'), pair 3, Fwd3 (5'- CCGCGGGCGTAAACGCTTCGAGATG -3'), Rev3 (5'- GGGAGACAG GGTGGGGGGTGG -3') with a High-Fidelity PCR kit (Invitrogen).

The PCR products were examined on 2% agarose gel and then purified using a PCR purification kit (Qiagen). PCR products were cloned into the pCR4-TOPO vector using the TOPO TA Cloning Kit for Sequencing (Invitrogen) as suggested by the manufacturer. 30 clones were picked for each prostate sample, grown and mini-prepped (Qiagen) and sent for sequencing using M13 Forward and M13 Reverse primers. Sequence data was collected on an ABI3730 automated sequencer. All sequence files were analyzed using DNA Strider 1.4f2.

Identification of function-inactivating missense mutations was as follows: protein missense mutations from mouse were aligned with the human p53 protein sequence to identify corresponding conserved residues. For the following steps the International Agency for Research on Cancer (IARC) TP53 database was used (http://www-p53.iarc.fr): conserved mutations were analyzed for 1) their identification in human cancer tissue, and 2) loss of more than 80% transactivation activity on p21 based on the published database (Kato S. *et al.*, Proc Natl Acad Sci USA 2003,*100*, 8424-8429) that used a reporter assay in yeast (data displayed on IARC TP53 database for each mutation).

Short hairpin and small interfering RNA

The short hairpin RNA against mouse *Phlpp1* (TCGAGAAGGTATATTGCTGTTGACAGTGAGCGCCAGAGAAACAGTTAATGATAATA

GTGAAGCCACAGATGTATTATCATTAACTGTTTCTCTGTTGCCTACTGCCTCGG) was generated on the basis of BIOPREDsi algorithms (Huesken D *et al. Nat Biotechnol* 2005;23, 995-1001.) and synthesized as a 110 bp oligo (Sigma), cloned into LMP (Dickins RA *et al. Nat Genet.* 2005; 37, 1289-1295.) and verified by sequencing. NIH3T3 cells were infected with shRNA-virus, and selected with 2 / ml puromycin to generate stable lines. Knockdown efficiencies of shRNAs were evaluated by using quantitative real-time PCR and western blotting**,** and the above most effective hairpin was used in all experiments. The short hairpin RNA against mouse *Phlpp2* were(shPhlpp2.1: TGCTGTTGACAGTGAGCGACTGAATCTAAGTGGGAACAAATAGTGAAGCCACAGAT GTATTTGTTCCCACTTAGATTCAGCTGCCTACTGCCTCGGA; shPhlpp2.2 TGCTGTTGACAGTGAGCGCGACAATGTTGATAGGAAATAATAGTGAAGCCACAGAT GTATTATTTCCTATCAACATTGTCATGCCTACTGCCTCGGA; shPhlpp2.3: TGCTGTTGACAGTGAGCGATTGGCTGTTACTGATAATGTATAGTGAAGCCACAGAT GTATACATTATCAGTAACAGCCAAGTGCCTACTGCCTCGGA) was designed, synthesized, and verified as described above.

NIH3T3 cells were infected with candidate shRNAs to determine knockdown efficiency by western blotting, and the most effective hairpins were used in all experiments. Primary MEFs were infected and selected as described above. shPten, shLuciferase and shp53 were kind gifts from Dr. Scott Lowe. siRNA Smart-pool (Dharmacon) against mouse Phlpp2 were transfected to MEFs at the final concentration of 50 nM using Dharmafect 1(Dharmacon) following the manufacturer's instruction.

Relapse free survival and scoring of TMAs

Disease recurrence after radical prostatectomy was defined as biochemical recurrence with PSA value greater than or equal to 0.2 ng/ml. Protein (from TMA), deletion, or RNA expression status was used to derive Kaplan-Meier curves on the subset of primary tumors that had clinical data on recurrence. A z-score threshold of 1.5 standard deviations was used to separate low (≤ -1.5) or high (≥ 1.5) from normal expression. For analysis of protein status, PTEN and PHLPP1 immunohistochemistry was performed on

a prostate cancer tumor tissue microarray with 114 evaluable cases in triplicate including normal tissue controls. PTEN and PHLPP1 staining was scored for each case as 0, +1, +2 by two reviewers. PTEN and PHLPP1 staining was considered negative with scores of 0 and 0/+1, respectively. All analyses for this publication were performed on de-identified patient data and material and thus qualified for exemption from human subjects statements under 45 CFR 46.101 (b) (4).

Statistical analysis of human metastasis data

For unbiased determination of significant co-deletions in metastatic samples mutual information was calculated for every pair of genes that was deleted at least 10 times (out of 37 samples) giving a total of >3000 genes (approximately 5 Mio pairs). False Discovery Rate analysis (Storey JD and Tibshirani R. *Proc Natl Acad Sci USA*. 2003 Aug 5;100(16):9440-5.) of the mutual information scores was carried out by first performing a Monte Carlo permutation test of the significance of each co-deleted pair of genes. The permutation test consisted of 100,000 random shuffles of the gene pair frequency data.

For visualization of the association of deletions in metastatic samples with *PTEN* or *PTEN*/ *PHLPP1* loss, paired whole genome comparisons were analyzed for significance (e.g. in PTEN normal vs. PTEN mutant metastases) using the Nexus Copy Number software (Biodiscovery, v. 5.1) where chromosomal regions reported as significantly different in aberration frequency in the two groups have met the minimum indicated p value based on a two tailed Fisher's Exact test as well as a minimum of 30 percent (Figure 6C) or 50 percent (Supplemental Figure S5D) difference in deletion frequency between the two groups. Areas of the genome with a statistically high frequency of aberration (indicated p value) were identified using the global frequency statistic approach of the STAC (Significance Testing for Aberrant Copy number) method (Diskin SJ et. al. *Genome Res.* 2006 16: 1149-1158) and the results were plotted using the Circos application (Krzywinski M et al., *Genome Res.* 2009 Sep;19(9):1639-45).